Scanning Microscopy

Volume 7 | Number 2 Article 23

3-31-1993

Use of Ultra-Thin Window Detectors for Biological Microanalysis

A. T. Marshall
La Trobe University

A. Patak
La Trobe University

Scanning Microscopy, Vol. 7, No. 2, 1993 (Pages 677-691)
Scanning Microscopy International, Chicago (AMF O'Hare), IL 60666 USA

0891-7035/93$5.00+.00

USE OF ULTRA-THIN WINDOW DETECTORS FOR BIOLOGICAL MICROANALYSIS

A.T. Marshall* and A. Patak

Analytical Electron Microscopy Laboratory, Department of Zoology,
La Trobe University,
Bundoora (Melbourne), Victoria 3083, Australia

(Received for publication November 30, 1992, and in revised form March 31, 1993)

Abstract

Films and bulk samples of Nylon, gelatin, Makrofol, epoxy resin, aminoplastic resin and sodium acetate have been used as models of biological samples. It is shown that the use of ultrathin window (UTW) detectors in scanning transmission and scanning electron microsopes permits the quantitative analysis of light elements, yielding a total element analysis with hydrogen estimated by difference or "guesstimated".

Comparison with known concentrations or concentrations obtained by chemical analysis shows that X-ray microanalysis of sections by the peak to continuum ratio model and bulk samples by the $\phi(\rho z)$ model gives sufficiently accurate results for biological purposes. It is also shown that sections may be analysed by the standardless ratio model.

The application of UTW detectors to total element analysis by quantitative elemental imaging is demonstrated of bulk biological samples, which have been freeze-substituted, embedded in epoxy resin and surface polished. The possibility of imaging the oxygen content of frozen-hydrated bulk tissue samples which have been surface polished is also demonstrated. This may lead to the imaging of water distribution in frozen-hydrated bulk samples of biological tissues.

UTW detectors are also useful for detecting mass loss in organic samples by monitoring the decrease in oxygen counts and for detecting contamination by monitoring the increase in carbon counts. It is also shown that changes in carbon counts are good indicators of folds in sections.

Key Words: Quantitative X-ray microanalysis, light element analysis, ultra-thin window detectors, biological, phi-rho-zed model, ZAF, peak to continuum ratio, ratio method, frozen-hydrated, thin sections, bulk samples.

*Address for correspondence:
Alan T. Marshall,
Department of Zoology, La Trobe University,
Bundoora, Victoria 3083, Australia
Telephone Number: (61) 03 479 2279
Fax Number: (61) 03 479 1188

Introduction

The feasibility of using windowless energy dispersive X-ray spectroscopy (EDXS) for light element detection in biological X-ray microanalysis was reviewed by Marshall (1984). Since that time significant advances in instrumentation have been made. These advances make the use of windowless (W) and ultrathin (UTW) detectors an almost routine possibility. UTW detectors are increasingly being used in preference to W detectors. There are several reasons for this preference. Throughput rates for light element X-rays have increased dramatically as a result of advances in pulse processor design and the consequent improvement in pulse pile-up rejection of low energy X-rays. As a result, detectors may now be positioned closer to the sample to take advantage of the increased solid angle of X-ray detection and thus increased count rate. With the closer positioning of the detector to the sample, the chances of light entering the detector are substantially greater. Light is generated by thermionic electron guns and reflected from the sample or sample holder or it is produced by cathodoluminescence of the sample. Photons entering the detector crystal produce noise which degrades the performance of the detector. UTW detectors are so called because they incorporate a shield of thin aluminium-coated polymer or self supporting aluminium foil which excludes photons.

UTW detectors should not be confused with atmospheric thin window detectors (ATW) which have "windows" of such materials as boron and silicon nitrides and diamond (Statham, 1991). These will support at least one atmosphere of pressure but do not have transmission properties for low energy X-rays which are comparable with UTW light shields.

The major advances have been in reducing electronic noise which limits the resolution of low energy X-ray peaks (Musket, 1986). This has largely been achieved by improvements in field effect transistor (FET) design and pulse processing (Statham and Nashoshibi, 1988). The limitations on operating conditions as outlined by Musket (1981, 1986) and Marshall (1984), however, are still valid. Modest count rates are still desirable even though pulse processing has greatly improved, and clean column environments are still

mandatory. At least one manufacturer now provides a facility for heating the detector crystal *in situ* to drive off water condensed as ice on the crystal. This allows the detection sensitivity for light elements to be easily maintained (Lowe, 1989) since the effect of the ice layer is to absorb low energy X-rays. Although this feature may allow some relaxation of the requirement for low amounts of water vapour to be present in the microscope column, it may not provide protection against hydrocarbon deposition which, as Musket (1986) points out, may cause leakage currents and a consequent degradation in resolution and peak shapes.

The use of a conditioning circuit for heating the detector crystal may also have benefits in "annealing" damage caused to the crystal by high energy electrons and X-rays (Lowe, 1989). High energy electrons and X-rays may cause hole traps to occur at the periphery of the detector crystal. This results in the subsequent drain of ionisation-induced electrons to the peripheral traps and thus incomplete charge collection. The physical manifestation of this is peak tailing in the spectrum. This type of damage can occur in the transmission electron microscope (TEM) and scanning transmission electron microscope (STEM) during low magnification operation when the magnetic field of the objective lens no longer constrains backscattered electrons. A high flux of high energy X-rays may also be damaging and can occur when a grid bar is irradiated during normal operation, i.e., not at low magnification. More permanent damage can be induced in which 'self counting' and resolution degradation are seen (Statham, 1991). Conditioning the detector crystal regularly often improves light element sensitivity. The reasons for this are obscure. It has been suggested that conditioning in a good vacuum may remove tenacious contaminants and that this is a reason for the observed improvement (L'Esperance *et al.*, 1990).

Advances in data processing have also occurred (Sevor *et al.*, 1989; Scott and Love, 1990) which suggest that light element analysis with commercially available software may be a more feasible proposition than hitherto. It will be shown here that acceptable results can be obtained from the analysis of organic materials of known composition. This suggests that biological analyses, where total elemental composition is required, will be feasible.

Light element analysis of biological or organic materials has not been extensive. Quantitative analyses of oxygen in organic materials have been accomplished by Marshall (1982), Marshall *et al.* (1985), Marshall and Condron (1987), and Marshall (1989) using a scanning electron microscope (SEM) and oxygen in coal has been analysed by Hemens *et al.* (1990) in a STEM. To date no light element analyses of organic materials have been made using a TEM or STEM as far as the present author is aware although inorganic materials have been analysed (e.g., Thomas, 1985) and a number of comparisons have been made between UTW energy dispersive X-ray microanalysis and electron energy loss spectroscopy of inorganic materials (e.g., L'Esperance *et al.*, 1990). A reason for detecting and quantifying oxygen in biological materials has been to devise a means of determining the water content of biological samples analysed as frozen-hydrated bulk samples (Marshall, 1982, 1987). This has allowed cellular ions to be expressed in terms of mmol l^{-1} of cell water, assuming that no ion binding to proteins or other cell constituents occurs.

However, if C, N and O can be detected and quantified, then it may be possible to greatly improve quantitative procedures for all elements. In analysing bulk biological samples in a SEM, it is a common practice to use "matching" standards. This is because commercial software employing matrix correction procedures generally only allows one unanalysable element to be calculated by difference and it has not proved satisfactory to use N as a representative of the undetectable matrix elements (Boekestein *et al.*, 1983). Total element analysis may also allow a straight forward calculation of elemental concentrations in sections from the Ratio Model (Russ, 1974) since the total of all the elements analysed must be 100 percent. Hydrogen is ignored or "guesstimated". A further benefit of UTW analysis of sections can be obtained when using the Peak/Continuum model since the matrix composition can be accurately calculated to obtain the matrix correction or G factor (Z^2/A) for the analysed sample.

A possible major benefit of UTW analysis of biological samples, however, is the potential for computing H_2O content from measurements of O concentrations in both bulk samples and sections. This entails the analysis of frozen-hydrated samples. In the case of bulk samples, the accuracy of the analysis of O will be improved if the sample is planed to a smooth "polished" surface. Topographical detail is then totally absent and the analysis must be conducted blind. A similar situation exists for frozen-hydrated sections. The only practical solution to this problem appears to be the use of quantitative X-ray imaging (Statham, 1988; Fiori *et al.*, 1988; Johnson *et al.*, 1988; Saubermann 1988; LeFurgey *et al.*, 1992). It is shown here that quantitative X-ray imaging is feasible in freeze-substituted bulk samples using a $\phi(\rho z)$ calculation to obtain correction factors based on an analysis of all elements present and that light element imaging is feasible in frozen-hydrated bulk samples. Using model systems, it is shown that quantitative light element analysis is possible in bulk samples and sections of organic material.

UTW detectors are also useful for assessing the flatness of a section surface and for monitoring contamination and mass loss. Section flatness is an important parameter since variations in section topography, i.e., folds, can go undetected visually and lead to erroneous analyses of sodium and magnesium in particular.

Quantitative Methods

Sections

The methods currently used for section analysis are Peak to Continuum Ratio, Peak Ratios and the Peak-

Volume (peripheral standard method) (reviewed by Hall, 1989). Of these the former two methods can be improved by UTW analysis, and UTW analysis could be used to verify the predicted elemental concentrations in the peripheral standard for the Peak-Volume method.

The Peak to Continuum ratio is formulated as:

$$C_{sp} = C_{st} \cdot \frac{I_{sp}/W_{sp}}{I_{st}/W_{st}} \cdot \frac{G_{sp}}{G_{st}} \quad (1)$$

where C = concentration as mass per unit mass, I = X-ray intensity for a particular element, W = continuum count, and G = relative efficiency of continuum generation and subscripts sp and st indicate specimen and standard respectively.

The matrix factor G is a function of atomic number and atomic weight and must be calculated from the composition. It is the weighted sum of Z^2/A for all the elements in the sample ($G = \Sigma((Z^2/A.C)$ where Z = atomic number, A = atomic weight and C = concentration for each element). G can be calculated iteratively during the processing of a spectrum if all elements are analysed, otherwise the standard procedure is to insert a "guesstimate" of the value.

Relative concentrations of elements can be obtained from the following equation (Russ, 1974):

$$C_1 : C_2 : C_3 : C_n = I_1/P_1 : I_2/P_2 : I_3/P_3 : I_n/P_n \quad (2)$$

where P is a proportionality constant.

If all elements are analysed, as is the case with a UTW detector, then

$$\Sigma C_{1\text{-}n} = 100\% \quad (3)$$

and a standardless analysis of the section is possible. The proportionality constants can be obtained from binary standards.

Bulk samples

The methods used for the analysis of bulk samples involve a comparison of the peak X-ray intensities from the sample with the peak X-ray intensities from standards with known elemental concentrations. A number of corrections must be made to account for the differences in generation and emission of X-rays if the sample matrix differs substantially from that of the standard. These corrections account for differences between sample and standard due to atomic number (Z), absorption of X-rays (A) and fluorescence of X-rays (F). These corrections are applied by means of the conventional ZAF model (Reed, 1975) or the $\phi(\rho z)$ model (Bastin *et al.*, 1984). The generic equation is:

$$C_{sp} = C_{st}.k/ZAF \quad (4)$$

where $k = I_{sp}/I_{st}$. Rough surfaced biological bulk samples have been analysed by a method in which ZAF corrections are applied to peak X-ray intensities normalised to the background under the peak (ZAF-PB method) (Statham and Pawley, 1978). This method is not suitable for light element analysis, however, because of the difficulties in estimating the background at very low energies (see Bloomfield and Love, 1985).

For light element analysis, the absorption correction may be of dominating importance. The classical ZAF procedures generally incorporate some form of Philibert's absorption correction (Philibert, 1963) which does not adequately account for the absorption of low energy X-rays (Scott and Love, 1990). The $\phi(\rho z)$ procedure (Parobek and Brown, 1978; Bastin *et al.*, 1984) can be expected to perform more accurate corrections for light element analysis and $\phi(\rho z)$ corrections have been used in biological analyses by Marshall (1982) and Marshall and Condron (1987).

The ionization function or $\phi(\rho z)$ curve describes the X-ray depth generation during electron excitation in a solid target (Reed, 1975). This function can be modelled by empirical equations. The absorption of generated X-rays by the matrix, as they are emitted from each depth interval, can be readily calculated and the combined atomic number and absorption correction obtained from the integrated value for the total emitted X-rays. The equation used for calculating elemental concentrations is:

$$C_{sp} = \frac{I_{sp}\int_0^{\infty} \phi(\rho z)\exp(-\mu \operatorname{cosec}\theta)d\rho z_{sp}}{I_{st}\int_0^{\infty} \phi(\rho z)\exp(-\mu \operatorname{cosec}\theta)d\rho z_{st}} \cdot C_{st} \quad (5)$$

where C is the concentration of the sample (sp) and standard (st), I is X-ray intensity, $\phi(\rho z)$ is the depth distribution for characteristic X-ray production, ρ is density, z is depth, θ is take-off angle and μ is the mass absorption coefficient.

Mass loss and contamination

Mass loss and contamination can compromise the accuracy of an analysis, particularly section analysis. Traditionally these phenomena have been observed by monitoring the continuum count rate (Hall and Gupta, 1974) or by other means such as monitoring the transmitted electron current (Marshall, 1980). However, the recorded signals are the sum of both mass loss and contamination and it is not possible to ascribe the observed signals unambiguously to one or the other phenomenon. By monitoring C and O counts, both events can be monitored since it appears that O is the element predominantly lost during mass loss, in resin embedded freeze-substituted tissue sections for example, whilst C is the element predominantly deposited during contamination.

Detection of folds in sections

The presence of folds in a section may compromise an accurate analysis, particularly the estimation of Na and Mg concentrations because of the effects on the absorption of Na and Mg X-rays.

The detection of folds in sections can be accomplished by making stereo-pairs of the section prior to analysis (LeFurgey *et al.*, 1992). This, however, can be

tedious and it may be difficult to match many high magnification fields with low magnification stereo-pairs when carrying out static beam analysis. An alternative approach is to carefully monitor the continuum count which will indicate absorption effects due to folding if an appropriate low energy continuum window is used. It will be shown that monitoring C counts is a much more sensitive indicator of folding.

Materials and Methods - X-ray Microanalysis Analytical Conditions

Scanning transmission electron microscopy (STEM)

X-ray microanalysis was performed with a Link LZ-5 ultrathin window energy dispersive detector (10 mm^2 in area) horizontally mounted on a JEOL 1200EX analytical STEM and a sample to detector crystal distance of approximately 25 mm. The detector was interfaced to a Link AN10000 processor and had a resolution of 133 eV FWHM at the Mn Kα peak. The electron microscope was operated at 120 kV in STEM mode with a large spot size. A hard X-ray aperture removed stray radiation. Under free lens control, the electron dose was $75x10^3$ e^-nm^{-2} for standards and $19x10^3$ e^-nm^{-2} for organic and biological specimens. This corresponds to a beam current of $1.0x10^{-9}$ A with a 200 second livetime and $0.5x10^{-9}$ A with a 100 second livetime, respectively, over an area of about 25 μm^2. These values take into account the difference between livetime and realtime, i.e., deadtime. The beam current was measured with a Faraday cup which could be inserted at the site of the hard X-ray aperture. This current represents the probe current incident on the specimen.

Specimens were analysed either at room temperature (25°C) in a carbon holder tilted at 25° towards the detector or at low temperature (-100°C) in an aluminium holder tilted 30° towards the detector. The microscope was operated with a liquid nitrogen cooled anticontamination device.

Scanning electron microscopy (SEM)

A Link energy dispersive LZ-5 X-ray detector with beryllium, ultrathin or windowless mode (30 mm^2 in area and a sample to crystal distance of 40 mm) was used mounted at 40° to the horizontal on a JEOL 840A analytical scanning electron microscope. The detector had a resolution of 140 eV and was interfaced to a Link eXL processor. Spectra were collected at 15 kV with an electron dose of 1.4 e^-nm^{-2} for standards except nitrogen which was analysed at 61 e^-nm^{-2} and organic specimens at 3.1 e^-nm^{-2}. This corresponds to a beam current of $0.5x10^{-10}$A for 100 second livetime over areas of 36700 μm^2, 830 μm^2 and 16300 μm^2, respectively. As before these values take into account the difference between livetime and realtime, i.e., deadtime. Beam, i.e., probe current was measured with a Faraday cup. Specimens were analysed at room temperature or on a low temperature stage at -170°C.

STEM - Standards

Thin crystals of pure binary salts were made by spraying a dilute aqueous solution onto copper grids filmed with pioloform after the method described by Hyatt and Marshall (1985). Salts insoluble in water were sprayed as an aqueous suspension. Grids were coated with 10 nm of aluminium or chromium. Deliquescent crystals were assumed to loose all free water in the column of the microscope. The standards for light elements were: commercially bought copper grids coated with carbon film; sprayed Si_3N_4 particles with an average diameter of 0.40 μm; and SiO_2 film on a titanium grid. These standards were used to produce a reference library of primary standards of all lines for each element, as well as secondary standards.

SEM - Standards

Primary as well as secondary standards were collected from commercially prepared microprobe standards (Biorad). However, the secondary standards for carbon, nitrogen and oxygen were obtained from aminoplastic resin (Roos and Barnard, 1984) which had been chemically analysed.

STEM - Correction procedures

The Hall peak to continuum method was used to process spectra (Hall, 1971). The Link software package Quantem.FLS applies a digital filter to the spectrum and fits library profiles to the peaks by linear least squares fitting to obtain peak intensities. The program uses FST factors (intensity correction factors) derived from secondary standards to calculate elemental concentrations.

$$FST_a = ((P_a/W)_{std}/C_{std}) \cdot G_{std} \qquad (6)$$

where P_a is the peak area of element 'a' after background subtraction, W is the area of continuum which spans from 1 to 20 keV in our case, C_{std} is the concentration of the standard in mmol kg^{-1} and G_{std} is the matrix correction for the standard. For all elements present:

$$G_{std} = \Sigma\ (CZ^2/A) \qquad (7)$$

where C is the concentration in mass fraction, Z is the atomic number and A is the atomic mass. The concentration of element 'a' in an unknown specimen (spec) is calculated by:

$$C_a = ((P_a/W)_{spec}/FST_a).G_{spec}. \qquad (8)$$

The total elemental composition needs to be known for an accurate estimate of G.

Spectra were processed using the ratio standard method (Cliff and Lorimer, 1975; RTS-2/FLS, Link software), with cobalt or rubidium as the standard (reference) element. Elemental sensitivity factors were calculated from experimentally determined sensitivity values obtained from binary standards with the peak to continuum method (Patak *et al.*, 1993). From Shuman *et al.* (1976), the ratio of peak to continuum counts is proportional to their molar proportions in a thin binary crystal of known composition A_MB_N.

$$k_{A-B} = \frac{(P/W)_B}{(P/W)_A} \cdot \frac{M}{N} = \frac{C_A}{C_B} \cdot \frac{k_B}{k_A} \quad (9)$$

where k_{A-B} = elemental sensitivity for element A with reference to element B, a constant; P/W = peak area to continuum area. The results of this equation will be in weight percent, however, results in molar ratios (or mmol kg^{-1}) can be obtained as follows:

$$^1k_{A-B} = \frac{(P/W)_B}{(P/W)_A} \cdot \frac{M}{N} \cdot \frac{A_B}{A_A} \quad (10)$$

where A is the atomic weight and ^1k is the elemental sensitivity value giving molar concentrations. Now

$$C_A \cdot C_B = \frac{M_A}{A_A} \cdot \frac{A_B}{N_B} \quad (11)$$

where C is the concentration in mmol kg^{-1}.

Also, using the peak to continuum method:

$$FST_A = \frac{P_A/W}{C_A} \cdot G_A \quad (12)$$

where P_A/W = peak area of element A over the continuum area (1-20 keV in our case); G_A = the matrix factor; C_A = the concentration of element A in mmol kg^{-1}, and FST is a standard factor.

It can be shown from equations (2) to (4) for compound A_MB_N that:

$$^1k_{A-B} = \frac{FST_B}{FST_A} \quad (13)$$

Furthermore,

$$^1k_{A-D} = {}^1k_{A-B} \cdot {}^1k_{B-C} \cdot {}^1k_{C-D} \quad (14)$$

Using equations (13) and (14) the elemental sensitivity constant was calculated for each element relative to rubidium. Absorption corrections were applied using Makrofol film as a mass thickness standard (Hall and Gupta, 1979).

SEM - Correction procedures

Two quantitative models were used: ZAF and $\phi(\rho z)$. These methods are for samples with a polished surface. The ZAF method (Reed, 1975) corrects for the following differential effects of sample and standard on the generation and emission of X-rays: the effect of atomic number on electron backscattering and slowing of penetrating electrons (Z); the effect of specimen composition and electron energy on absorption of X-rays (A); a correction for X-rays produced by primary electron excited X-rays (fluorescence, F). The effect of F is small. The concentration of an element (C_{sp}) is calculated by:

$$C_{sp} = C_{st} \cdot k/ZAF \quad (15)$$

where $k = I_{sp}/I_{st}$, and I is the peak area. The Link ZAF4 program employs the Philibert (1963) absorption correction model and the mass absorption coefficients of Heinrich (1987), the atomic number correction of Duncumb and Reed (1968) and the characteristic fluorescence correction of Reed (1965).

The Link $\phi(\rho z)$ method is based on the model by Bastin *et al.* (1984) which uses a modified Gaussian function to obtain Z and A corrections:

$$ZA = \frac{\int_0^\infty \phi(\rho z)\exp(-\chi\rho z)d\rho z_{sp}}{\int_0^\infty \phi(\rho z)\exp(-\chi\rho z)d\rho z_{st}} \quad (16)$$

where sp is the specimen and st is the standard and $\chi = \mu\text{cosec}\theta$ where μ is the mass absorption coefficient and θ is the take-off angle.

X-ray Imaging of Specimens in SEM

Qualitative X-ray images

The area to be imaged was selected and a secondary electron image stored. A spectrum previously collected from the specimen was used to select peak and continuum areas of similar width. Elemental and continuum images were then collected using these windows from the spectrum. The areas of continuum were selected close to the peaks of interest, so as to approximate the continuum under the peak as closely as possible. Beam current was 5.0×10^{-10} A with a dwell time of 5 milliseconds; 20 frames were collected at a resolution of 128x128 pixels. Images were processed by subtracting continuum maps from peak maps.

Quantitative X-ray images

Quantitative X-ray images were obtained using a dwell time of 1 to 5 seconds, only 1 frame at a resolution of 128x128 pixels was collected. Images were processed with $\phi(\rho z)$ corrections obtained from appropriate rastered areas of the sample using the static beam analysis programs. The elements to be imaged were defined beforehand, and standard deviation maps were collected for elements which were present in rather low concentrations. The standard deviation maps were used to reduce noise by setting to zero pixels with values less than one, or more, standard deviations. The X-ray images were thus corrected at every pixel but only by 'averaged' correction factors. There is thus an inherent degree of inaccuracy due to specimen inhomogeneity. However, since the biological structures are embedded in a permeating matrix of either resin or ice, the inaccuracies are assumed not to be great since the average atomic number will not vary greatly in most cases.

Light Element Tests

The accuracy and reliability of quantitative light element analysis in STEM and SEM were assessed using various compounds whose composition was either well known, or was determined by chemical analysis. The composition of sodium acetate and Spurr's resin was

calculated, that of Makrofol was obtained from Hall and Gupta (1979), and aminoplastic resin, gelatin, Nylon and albumin were chemically analysed. Spurr's resin was prepared using the chlorine-free formulation of Pallaghy (1973) and incorporating potassium into the resin using kryptofix 222 (Merck) according to Roomans (1979) and Condron and Marshall (1986). Gelatin was prepared as a 20% dialysed solution cast into Petri dishes and dried in an oven at 60°C to constant weight. Nylon samples were prepared from planed Nylon chips (Dupont, Elvamide) and aminoplastic resin was prepared by a slight modification of the methods of Roos and Barnard (1984) and Morgan and Winters (1989). Albumin, Makrofol and sodium acetate were analysed only in STEM. The others were analysed in STEM and SEM; where possible, the section and bulk sample analysed came from the same piece of material.

STEM

Albumin and sodium acetate samples were prepared by spraying a dilute aqueous solution onto heated copper grids filmed with pioloform. Aminoplastic and Spurr's resin specimens were analysed as 1 μm sections which had been cut dry and placed on copper grids filmed with pioloform. Gelatin was prepared by dipping grids into a 20% aqueous solution of gelatin (Sumner, 1990). Other grids were filmed with a thick Nylon film (Echlin and Moreton, 1974). A 2 μm thick film of Makrofol was placed onto a naked copper grid. Albumin, aminoplastic resin, Spurr's resin, gelatin and Nylon were coated with 10 nm aluminium and analysed at -100°C; this reduced mass loss and contamination. Sodium acetate crystals which were coated with 10 nm aluminium, were analysed at 25°C as was Makrofol.

SEM

Aminoplastic, Spurr's resin and Nylon specimens were planed on a microtome and glued onto an aluminium stub with colloidal carbon. The stubs were coated with 10 nm aluminium and analysed at 25°C.

Evaluation of Analyses

Evaluation of light element analyses was accomplished by determining the root mean square (rms) percent error and average ratio of measured (M) to known (k) concentrations.

$$rms = 100 \cdot \sqrt{\frac{\sum_{i=C,N,O} \left(\frac{M_i - k_i}{k_i} \right)^2}{n}} \qquad (17)$$

$$average\ ratio = \frac{\sum_{i=C,N,O} \frac{M_i}{k_i}}{n} \qquad (18)$$

where C, N, O, are elements C, N and O and n is the number of elements.

Preparation of Biological Specimens

Malpighian tubules

Malpighian tubules were dissected from freshly killed adult male black field crickets (*Teleogryllus oceanicus*). A small portion of the tubules was removed and placed on an aluminium pin. The tubules were frozen using a Reichert-Jung KF80 freezing device by plunging the pin into liquid propane at -190°C cooled with liquid nitrogen. The frozen tubules were polished on the pin by cutting ultrathin sections in a Reichert-Jung FC4E cryoultramicrotome. The pin was then mounted in a substage and the tubules were coated with 10 nm aluminium at -170°C. The substage was transferred to a Biorad (MK3) liquid nitrogen cold stage in the SEM and held at -170°C during microanalysis.

Coral samples

Small coral polyps (*Galaxea fascicularis*) were frozen by plunging into liquid nitrogen-cooled propane at -190°C, freeze-substituted in ether/acrolein and embedded in Cl-free Spurr's resin. Slices of the polyps were cut with a diamond saw, mounted on stubs with colloidal carbon and coated with 10 nm aluminium. Details of the procedures are given in Marshall (1980) and Marshall and Wright (1991). The samples were transferred to the SEM and analysed at ambient temperature.

Rat kidneys

Rat kidneys were prepared in a similar manner to the coral samples except that dry-cut sections 1 μm thick were placed on grids for STEM analysis.

Results

UTW analyses in STEM

Test samples in which the composition was either known by calculation or by chemical analysis were analysed as films (Nylon, gelatin and Makrofol) or as sections (epoxy resin, amino-plastic resin) or as sprayed microdroplets (sodium acetate). A typical spectrum is shown in Figure 1.

The correspondence between calculated or chemically analysed elemental compositions of the samples and the elemental concentrations determined in STEM by the peak to continuum model was good when an average assumed value for H was included and the data normalised (Table 1). The assumed value is derived from Engström (1966) as 7% for an average protein. The percentage differences between known and measured concentrations are shown in Table 2.

A standardless analysis using the Ratio model was carried out, following which the concentrations were normalised after an assumed value for H concentration was included. The analytical concentrations are in good agreement with those obtained by chemical analysis (Table 1). A comparison of the two models applied to Nylon is illustrated in Figure 2. The overall error and accuracy of the STEM analyses are indicated in Table 3.

Table 1. Analysis of organic compounds in STEM using the Hall peak to continuum (P/W) ratio method and the Ratio method. Concentrations (mean ± standard deviation, SD) are normalised weight percentages assuming that H is 7%.

Compound	Method	Element				
		H	C	N	O	Other
Albumin	Chemical	6.7	47.1	14.4	29.5	2.6 (S)
	P/W (10*)	7.0	46.1 ± 2.5	15.9 ± 2.8	28.9 ± 2.1	2.0 ± 0.4
	Ratio (10)	7.0	47.5 ± 2.3	12.8 ± 2.3	31.3 ± 2.2	1.4 ± 0.3
Aminoplastic	Chemical	7.0	39.4	29.6	23.9	
	P/W (8)	7.0	37.8 ± 0.5	31.7 ± 0.6	23.5 ± 0.4	
	Ratio (8)	7.0	40.2 ± 0.5	26.3 ± 0.5	26.4 ± 0.5	
Gelatin	Chemical	6.5	45.2	16.5	31.5	
	P/W (10)	7.0	42.6 ± 0.6	21.2 ± 0.4	29.2 ± 0.2	
	Ratio (10)	7.0	44.0 ± 4.1	17.1 ± 2.1	31.8 ± 2.1	
Makrofol	Calculated	6.0	76.0	0.0	19.0	
	P/W (8)	7.07	71.4 ± 0.6	0.1 ± 0.2	21.5 ± 0.4	
	Ratio (8)	7.0	70.5 ± 0.5	0.1 ± 0.1	22.4 ± 0.4	
Nylon	Chemical	9.4	60.9	11.0	18.4	
	P/W (10)	7.0	60.2 ± 1.0	14.0 ± 0.5	18.8 ± 0.6	
	Ratio (10)	7.0	58.6 ± 1.0	15.2 ± 0.5	19.5 ± 0.6	
Na acetate	Calculated	4.0	30.0	0.0	38.0	28.0 (Na)
	P/W (5)	7.0	25.5 ± 2.9	0.4 ± 0.4	38.0 ± 2.9	29.1 ± 1.1
	Ratio (5)	7.0	28.0 ± 4.2	0.3 ± 0.3	43.7 ± 2.0	21.0 ± 2.4
Spurr's resin	Calculated	9.0	69.0	0.4	22.0	0.4 (K)
	P/W (8)	7.0	66.6 ± 0.6	0.0	26.4 ± 0.6	0.5 ± 0.2
	Ratio (8)	7.0	65.6 ± 0.7	0.0	27.4 ± 0.7	

*(n) = number of analyses.

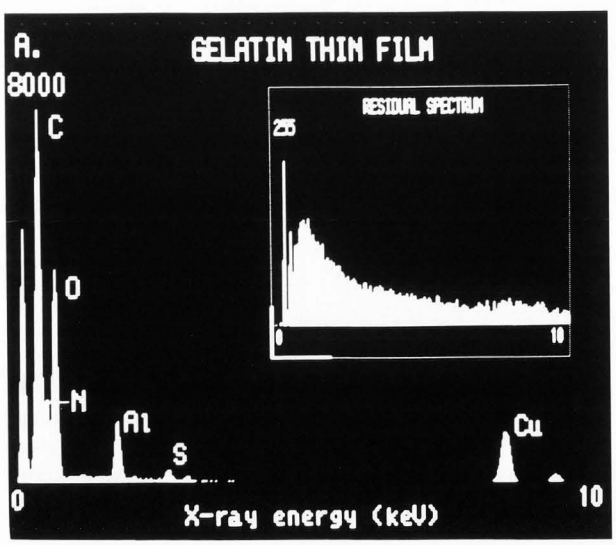

Figure 1. Spectrum from a thin film of gelatin obtained with a UTW detector. The residual continuum after peak fitting and removal is shown.

Table 2. Percentage deviation of concentration measurements by the Hall peak to continuum method.

Compound	Element		
	C	N	O
Albumin	+2.0	+11.0	-2.0
Aminoplastic	-4.8	+7.4	-1.7
Gelatin	-6.0	+29.0	7.0
Makrofol	6.0		+14.0
Nylon	-1.0	+27.0	+2.0
Na acetate	-14.0		-1.0
Spurr's resin	4.0		+20.0

UTW analyses in SEM

Bulk samples of epoxy resin, Nylon and gelatin were analysed using the $\phi(\rho z)$ and ZAF4 models. Samples were analysed with hydrogen as the unanalysed element, i.e., hydrogen concentration was calculated by the difference of the sum of the percentage concentrations of the other elements from 100. The results are shown in Table 4. It is clear that the correspondence between

Table 3. Comparison of several correction procedures.

Method	root mean square (rms) error (%)						
	albumin	aminoplastic	gelatin	makrofol	nylon	Na acetate	epoxy
P/W	54.4	25.0	49.8	12.8	38.5	45.3	42.4
P/W normalised	6.3	4.8	17.3	10.4	16.0	10.6	14.5
Ratio	7.4	8.9	2.7	13.8	21.8	11.6	17.9
ZAF			26.2		80.1		42.5
PhiRhoZed		17.5		3.7		16.1	
Method	average ratio						
	albumin	aminoplastic	gelatin	makrofol	nylon	Na acetate	epoxy
P/W	1.54	1.24	1.44	0.90	1.35	1.44	1.40
P/W normalised	1.02	1.00	1.05	1.04	1.09	0.93	1.08
Ratio	0.99	1.01	1.01	1.05	0.89	1.04	1.10
ZAF			1.23		1.53		1.31
PhiRhoZed			1.17		0.99		1.05

Table 4. Analysis of organic compounds in SEM using ZAF and $\phi(\rho z)$ models and designating H as the unanalysed element. Concentrations are expressed as weight percentages (mean ± SD).

Compound	Method	Element				
		H	C	N	O	K
Gelatin	Chemical	7	45	17	32	
	ZAF (5*)	0	63 ± 6.4	18 ± 1.0	38 ± 1.6	
	$\phi(\rho z)$ (5)	0	51 ± 0.9	20 ± 0.7	37 ± 0.9	
Nylon	Chemical	9	61	11	18	
	ZAF (5)	0	143 ± 46	10 ± 1.5	24 ± 1.4	
	$\phi(\rho z)$ (5)	9	63 ± 1.7	11 ± 0.6	17 ± 0.7	
Spurr's resin	Calculated	9	69	0.4	22	0.39
	ZAF (5)	0	10.2 ± 12	0	30 ± 3.0	0.42 ± 0.07
	$\phi(\rho z)$ (5)	0	70 ± 0.3	0	27 ± 0.3	0.35 ± 0.06

* (n) = number of analyses.

known and measured concentrations is reasonable except in the case of C concentrations obtained by application of the ZAF model. A comparison of the models applied to Nylon is shown in Figure 3. Correspondence between known and measured concentration in Nylon obtained by the $\phi(\rho z)$ model is very good but the correspondence is not so close in the case of gelatin for all elements and for O in epoxy resin. The percentage differences between known and measured concentrations are shown in Table 5. If the results for gelatin are normalised, then the correspondence increases markedly and even further if the concentration of H is assumed to be the value (7%) found in a protein of average elemental composition (Engström, 1966) (Table 6). The overall error and accuracy of the SEM analyses are indicated in Table 3.

Mass loss and contamination in sections

Mass loss and contamination were induced during analysis of an epoxy resin section of freeze-substituted rat kidney by conducting the analysis with a high electron dose and without a liquid nitrogen cooled anticontamination device. The count rate was recorded every 5 seconds for C, O, K windows and a continuum band. In Figure 4, it can be seen that O counts decrease steeply in the initial 20 seconds whereas C counts increase steadily over the period of the analysis. The decline in O counts may be attributed to mass loss whereas the

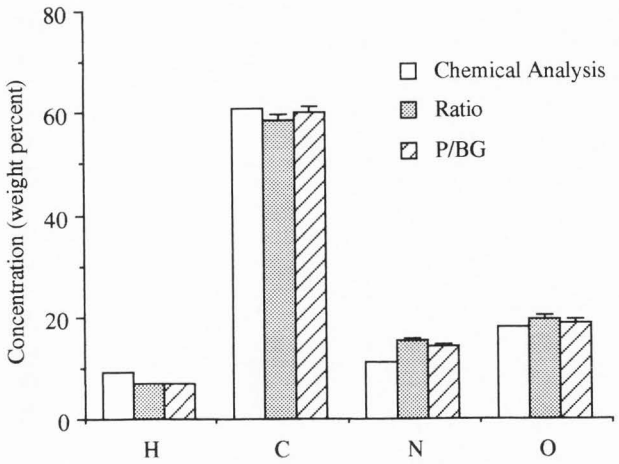

Figure 2. Comparison of analyses of Nylon films using the Ratio and Peak to Continuum models. Mean + standard error (SE), n = 10.

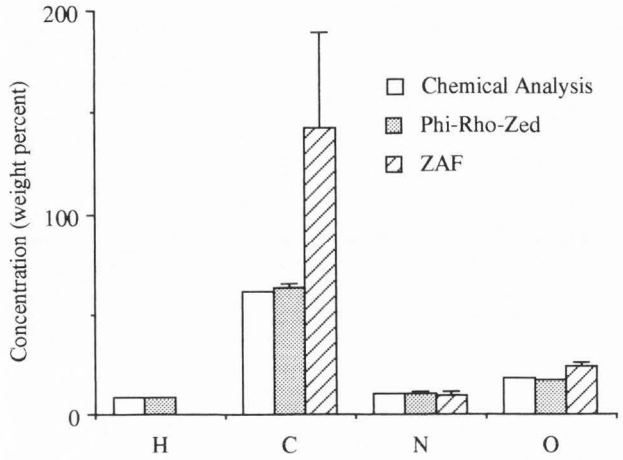

Figure 3. Comparison of analyses of Nylon bulk samples using the $\phi(\rho z)$ and ZAF models. Mean + SE, n = 5.

Table 5. Percentage deviation of concentration measurements by $\phi(\rho z)$ and ZAF models from known concentrations.

Model	Element	Nylon	Epoxy resin	Gelatin
Phi-Rho-Zed	H	0	-78	
	C	+3.3	+1.4	+13.3
	N	0	0	+17.6
	O	-5.6	+22.7	+15.6
ZAF	H			
	C	+134	+47.8	+40
	N	-9	0	+5.9
	O	+33	+36.4	+18.8

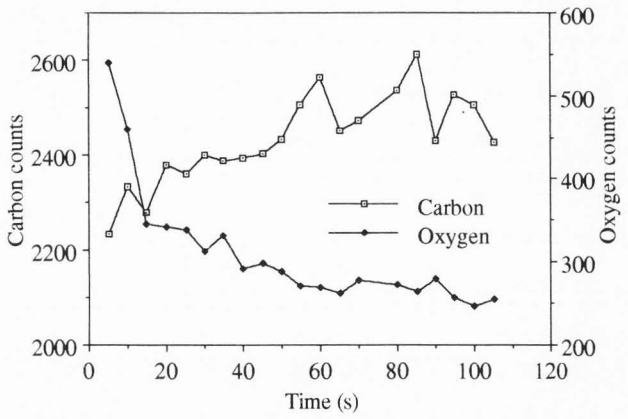

Figure 4. STEM analysis of freeze-substituted rat kidney showing changes in C and O counts with time as a result of contamination and mass loss respectively.

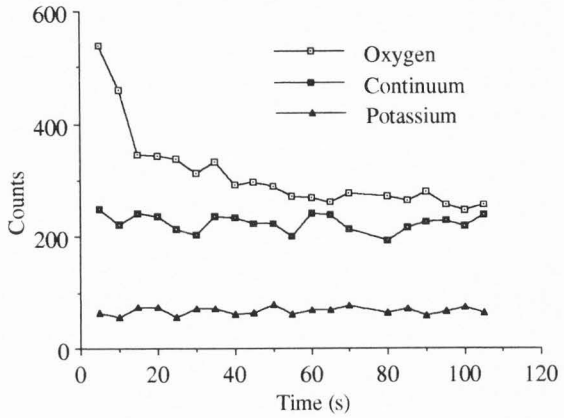

Figure 5. STEM analysis of freeze-substituted rat kidney showing that O counts decrease as a result of mass loss but continuum and K counts remain constant.

---

increase in C counts may be attributed to contamination. An inspection of continuum and K counts (Fig. 5), however, does not reveal any indication of either mass loss or contamination. Coincidentally, the processes of mass loss and contamination negate each other so that their effects are undetectable by an inspection of continuum count rate or a contained element such as K.

Detection of folds in sections

In a section of uniform thickness, flatness and chemical homogeneity, there should be a linear relationship between characteristic and continuum X-rays and beam current. Such a relationship was obtained with flat sections of aminoplastic resin for C, N, O and continuum (Fig. 6). Figure 6 shows X-ray counts at different beam currents and at different locations on the section. A similar analysis carried out on a section with folds gave the results shown in Figure 7. The effect of folds at different locations on the section has a marked influence on X-ray counts with C showing the greatest sensitivity.

Table 6. Elemental concentrations of gelatin determined by $\phi(\rho z)$ model and adjusted by normalisation and inclusion of an 'average' value for H concentration.

Element	Chemical analysis	Phi-Rho-Zed	Normalised	Average H and normalised	Percentage difference
H	7	0	0	6	-14
C	45	51	47	44	-2
N	17	20	18	17	0
O	32	37	34	32	0

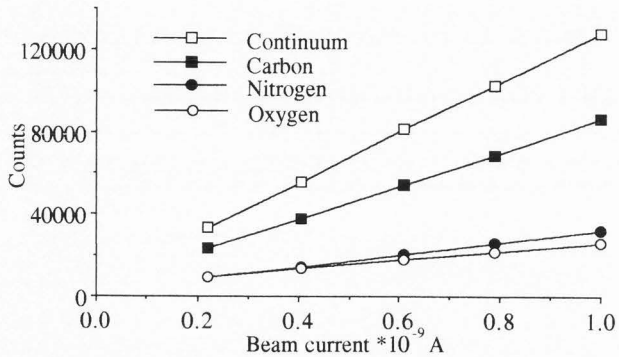

Figure 6. STEM analyses of a flat aminoplastic resin section at increasing beam currents showing the expected linear increase in counts for continuum (1-20 keV), C, N and O.

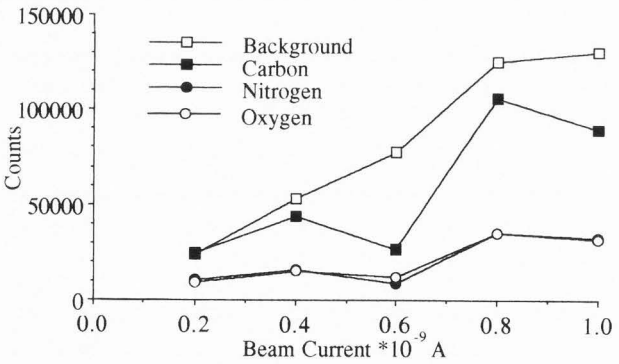

Figure 7. STEM analyses of an aminoplastic section with folds at increasing beam currents showing that continuum (1-20 keV), C, N and O counts do not increase in a linear manner due to absorption effects.

A comparison of the sensitivity of different continuum bands to folds is shown in Figures 8 and 9. Continuum of different energies varies in its response to folds but none of the energy bands was as sensitive as C.

Quantitative X-ray imaging

Preliminary selected area (static beam) analyses were carried out on a cross-section of freeze-substituted coral epithelium cut with a diamond saw. Application of

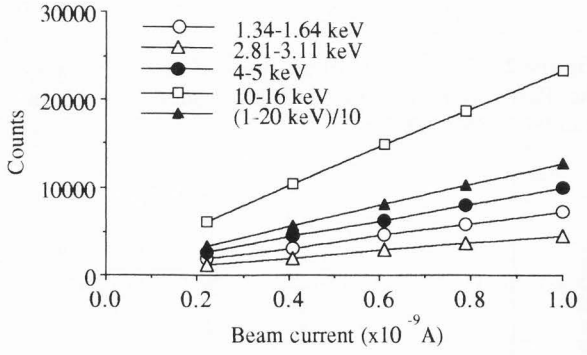

Figure 8. STEM analyses of a flat aminoplastic section at increasing beam currents showing linear increases in counts from different regions of the continuum.

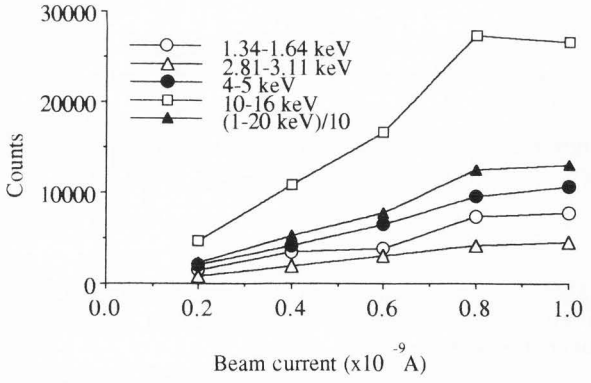

Figure 9. STEM analyses of an aminoplastic section with folds at increasing beam currents showing that the increase in counts from different regions of the continuum is very variable.

---

the $\phi(\rho z)$ model provided average correction factors for elemental images. The quantitative X-ray images (Fig. 10) yielded concentration values for various elements associated with mucocytes in the epithelia. These values are comparable with concentrations obtained from sections of similar specimens using the peak to continuum model (Marshall and Wright, 1991).

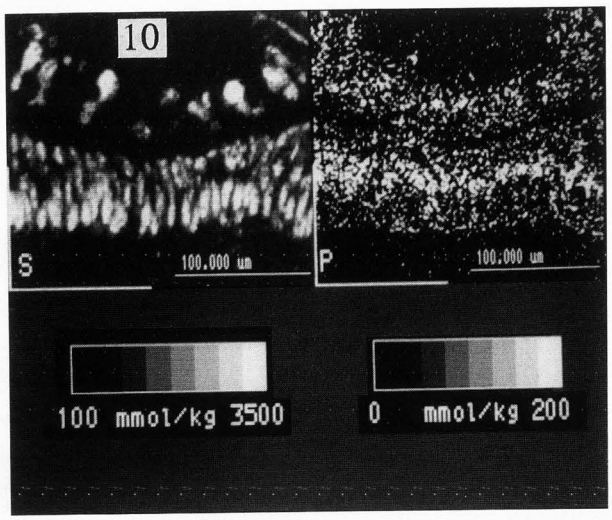

Figure 10. Quantitative elemental images from freeze-substituted coral epithelia obtained from bulk samples in a SEM by application of the $\phi(\rho z)$ model. The distributions of S in mucocytes and P in all epithelial cells are shown.

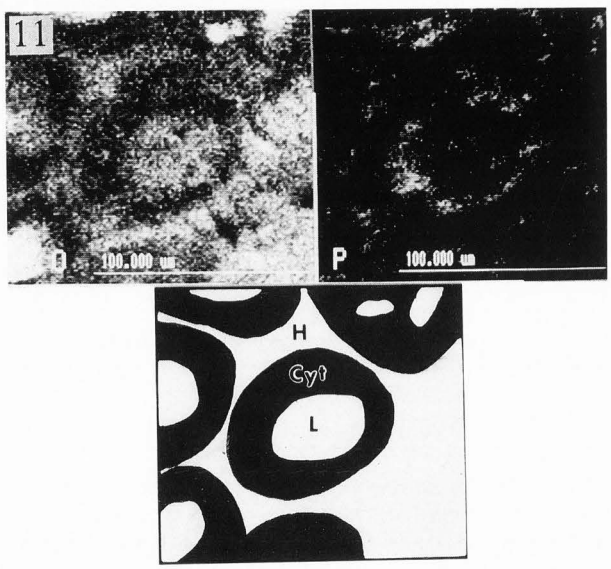

Figure 11. Qualitative elemental images obtained in SEM from frozen-hydrated bulk samples of cricket Malpighian tubules. The differential distribution of O between cytoplasm (Cyt) and fluids in haemolymph (H) and lumen (L) has been made obvious by exaggerating the contrast. The distribution of P in intracellular calcium phosphate spherites confirms the identification of the cell cytoplasm in the O image.

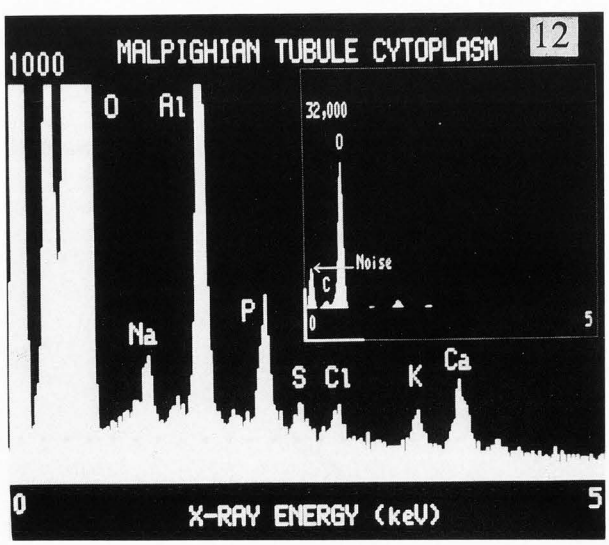

Figure 12. UTW X-ray spectrum from cytoplasm of frozen-hydrated Malpighian tubule cells prepared as a polished bulk sample and analysed in SEM.

Qualitative X-ray imaging of frozen-hydrated specimens

As an initial step towards quantitative light element imaging of frozen-hydrated samples, it first needs to be shown that meaningful images of light elements can be obtained from featureless, polished or planed, biological samples. For this purpose, a preparation of insect Malpighian tubules was chosen because these have regular easily recognised profiles. The cytoplasm contains spherites of calcium phosphate which can be recognised in backscattered electron images and thus provides a guide in an otherwise featureless polished surface. The tubules also contained an aqueous fluid in the lumina and were surrounded by haemolymph. It was anticipated that these two phases would be distinguishable from the cytoplasm by virtue of the differences in C and O concentrations. It is shown in Figure 11 that the higher O concentration in frozen fluid can be distinguished from cell cytoplasm where the O concentration is lower. This is clearly seen by comparison of the O image and P image, the latter being predominantly from intracellular spherites. Potassium and C are present in relatively much lower concentrations and require longer imaging times to provide clear elemental images. The much higher intensity of the O peak relative to the other intracellular elements is illustrated in Figure 12.

Discussion

Previous attempts to use energy dispersive spectrometers for quantitative analysis of light elements have relied on background subtraction techniques prior to the determination of peak areas. These have involved either subtracting a background generated from a light element material such as Be (Marshall, 1984) or subtracting a calculated background (Bloomfield and Love, 1985). In addition, the electronic noise peak at zero energy and other spectral artefacts had to be dealt with. Further, difficulties were encountered in peak fitting because of the low energy tails, resulting from incomplete charge collection, present on low energy peaks.

In the present investigation, the application of digital filtering and least-squares fitting of library spectra to obtain peak integrals (Statham, 1984) appears to be satisfactory. This may be due in part to the improvements in low energy peak shape and resolution. The electronic noise peak is treated in the same way as a characteristic X-ray peak (Statham, 1986).

The effectiveness of spectrum processing is reflected in the quantitative results. In general, the quantitative correspondence between the X-ray analytical and chemically analysed or calculated values for a range of organic compounds of well defined stoichiometry is good and is adequate for analyses of biological samples. However, acceptable results are only reproducibly obtained in STEM analyses when a "guesstimate" of H concentration (derived from the H content of a generalised protein) is taken into account and the analytical concentrations are normalised. The need for normalisation indicates that there are unidentified factors causing a degree of error in some analyses of some materials.

Analyses were carried out on bulk samples at 15 kV because this appears to be the optimum accelerating voltage for the analysis of frozen-hydrated biological bulk samples (Marshall, 1982). At this accelerating voltage, the depth resolution for all elements of biological interest is similar. However, the absorption corrections for C, N and O under these conditions are considerable which, therefore, represent a severe test of the matrix correction procedures.

The problem of absorption correction in biological matrices has been discussed by Roomans (1981), Marshall (1982) and Boekestein *et al.* (1983). The classical ZAF correction program (ZAF4) of the Link software package uses an absorption correction based on that of Philibert (1963) and did not give accurate results for C in particular.

Because of the high C values obtained, it was not possible to obtain a value for H as the unanalysed element. Some improvement in the ZAF results could be expected (Sevov *et al.*, 1989) if the absorption correction of Sewell *et al.* (1985) was used in the ZAF model. In comparison, the ϕ (ρz) model (Bastin *et al.*, 1986) performed well for all light elements with root mean square (rms) error values better by 8.7% for gelatine, 26.4% for epoxy resin and 76.4% for Nylon. The average ratios were also considerably improved. It was possible to obtain an estimate of H concentration as the unanalysed element. Previous attempts to carry out light element analyses of biological samples were restricted to determining O concentrations in order to calculate the H_2O content of cells (Marshall *et al.*, 1985; Marshall, 1989). At this time, C could not be adequately discriminated from the noise peak to make quantitation of C entirely feasible. The present results suggest that measurements of C and O concentrations in frozen-hydrated samples will now be possible. Preliminary analyses (Marshall, unpublished) indicate that this is indeed the case. Previous analyses of O have been carried out on fractured surfaces of frozen-hydrated bulk samples with the necessity of inspecting a back-scattered electron image from a BE detector mounted on the X-ray detector in order to select a flat, horizontal surface suitable for analysis. Whilst this method has given acceptable results for O in frozen-hydrated samples, the estimation of relatively much lower C concentrations would be more succeptable to error. An alternative approach is digital quantitative X-ray imaging (Statham, 1988; LeFurgey *et al.*, 1992).

This technique has not so far been applied to light elements in bulk samples or to sections in the frozen-hydrated state, For bulk sections, it would require a polished or planed surface. As a consequence, the analysis must be carried out blind since the sample will be structurally featureless in the electron image. The preliminary qualitative X-ray images on such samples shown in this investigation suggest that this approach may be feasible. Quantitative images for higher atomic number elements obtained from featureless resin blocks further indicate the utility of this approach. These latter images are the result of correcting elemental images of apparent concentration (i.e., the product of standard concentration and the ratio of characteristic peak intensities from specimen and standard) by applying the appropriate $\phi(\rho z)$ matrix correction factors pixel by pixel.

In sections, the Hall peak to continuum model produces acceptable results for light element analyses only after normalisation and this is further improved if a "guesstimate" for H concentration is included. The results after this procedure are excellent, showing a considerable reduction in the rms error and in the average ratio. The cause of the inaccuracies which make normalisation necessary has not so far been identified but it may well relate to the nature of the continuum at the low energy end of the spectrum.

The Hall peak to continuum model requires that extraneous continuum should be accounted for (Roomans, 1980; Nicholson *et al.*, 1982; Hall, 1989) and the method also requires standards. An alternative possibility is the Ratio method (Cliff and Lorimer, 1975; Russ, 1974) which has been used in biological analyses for obtaining relative concentrations of elements. This method requires no standards other than those required to obtain the proportionality factors relating the efficiency of X-ray generation and detection of one element to another. The method is also independent of extraneous continuum generation. If the analysis is a total elemental analysis, then the absolute concentrations of elements can be obtained. This is a procedure in common use in materials science but has not previously been used in biological analyses since a knowledge of the light element concentrations is normally lacking. The present results indicate that the Ratio method may be applicable to biological samples if a "guesstimate" of H concentration is included and if the concentrations are normalised. The method has the advantage of simplicity and does not require standards. The present results are comparable with those obtained from the peak to continuum ratio method.

The analysis of sections may be confused and confounded by undetected mass loss and/or contamination and by undetected folds in sections. Mass loss and contamination may be monitored by observing the continuum rate (Hall and Gupta, 1974) or by monitoring the transmitted electron current (Marshall, 1980) although if one compensates the other, no change in either continuum or transmitted electron current may be observed.

An alternative and more certain method is to observe the C and O counts as shown here. Mass loss from organic samples appears to frequently, if not invariably, involve a loss of O whereas contamination is seen as a deposition of C.

Folds in sections may be detected by inspecting stereopairs (LeFurgey *et al.*, 1992) of the sample or possibly by observing a continuum line scan signal or backscattered electron line scan signal. However, the C signal, as shown here, is extremely sensitive to changes in local topography due to absorption. Thus, an inspection of the changes in C and O counts from one static beam analysis to another in a section will often reveal the effects of unobserved folds after the analyses have been completed. Although not yet tested, it is probable that similar changes in C and O counts in X-ray images would also be a good indicator of fold effects. This may be particularly useful in interpreting data from freeze-dried cryosections which often do not lie flat on grids.

Conclusions

Modern pulse processing technology allows a sufficiently high count rate to be obtained to facilitate simultaneous analysis of biological samples containing high Z elements in low concentrations and low Z elements in high concentration. Spectrum deconvolution by means of filtered least squares fitting enables peak integrals for low Z elements such as C, N and O to be accurately obtained from the well shaped and well separated peaks obtained by modern pulse processors.

Quantitative light element analysis of bulk samples of organic samples is possible with commercial $\phi(\rho z)$ programs but not with ZAF programs which use the simple Philibert (1963) absorption correction. Quantitative light element analysis is also possible in sections using the Peak to Continuum model although results have to be normalised which indicates that some unidentified cause of error in the procedure exists. Standardless analyses of light element matrices using the Ratio Method is also possible.

Acknowledgements

The authors are grateful to Dr B.L. Gupta for the gift of Makrofol film and to Dr A. Wright and L. Dalton for technical assistance. This work was supported by a grant from the Australian Research Council.

References

Bastin GF, van Loo FJJ, Heijligers HJM (1984) An evaluation of the use of Gaussian $\phi(\rho z)$ curves in quantitative electron probe microanalysis. A new optimisation. X-ray Spectrom **13**: 91-97.

Bastin GF, Heijligers HJM, van Loo FJJ (1986) A further improvement in the Gaussian $\phi(\rho z)$ approach for matrix correction in quantitative electron probe microanalysis. Scanning **8**: 45-67.

Bloomfield DJ, Love G (1985) Quantitative light element analysis using an energy-dispersive detector. X-ray Spectrom **14**: 8-15.

Boekestein A, Stadhouders AM, Stols ALH, Roomans GM (1983) Quantitative biological X-ray microanalysis of bulk specimens: an analysis of inaccuracies involved in ZAF correction. Scanning Electron Microsc **1983**;II: 725-736.

Cliff G, Lorimer GW (1975) The quantitative analysis of thin specimens. J Microsc **103**: 203-207.

Condron RJ, Marshall AT (1986) Inhomogeneity in epoxy resin standards for quantitative biological X-ray microanalysis. J Microsc **143**: 249-255.

Duncumb P, Reed SJB (1968) The calculation of stopping power and backscatter effects in electron probe microanalysis. In: Quantitative Electron Probe Microanalysis. Heinrich KFJ (ed.). Natl Bur Stand Spec Publ **298**, US Dept of Commerce, Washington DC. pp. 133-154.

Echlin P, Moreton R (1974) The preparation of frozen-hydrated biological material for X-ray microanalysis. In: Microprobe Analysis as Applied to Cells and Tissues. Hall T, Echlin P, Kaufmann R (eds.). Academic Press. pp. 159-174.

Engström A (1966) X-ray microscopy and X-ray absorption analysis. In: Physical Techniques in Biological Research. Pollister AW (ed.). Academic Press. pp. 87-171.

Fiori CE, Leapman RD, Swyt CR, Andrews SB (1988). Quantitative X-ray mapping of biological cryosections. Ultramicroscopy **24**: 237-250.

Hall TA (1971) The microprobe assay of chemical elements. In: Physical Techniques in Biological Research. Vol. 1(c). Oster G (ed.). Academic Press. pp. 157-175.

Hall TA (1989) Quantitative electron probe X-ray microanalysis in biology. Scanning Microsc. **3**: 461-466.

Hall TA, Gupta BL (1974) Beam-induced loss of organic mass under electron microprobe conditions. J Microsc **100**: 177-188.

Hall TA, Gupta BL (1979) EDS quantitation and application to biology. In: Introduction to Analytical Electron Microscopy. Hren JJ, Goldstein JI, Joy DC (eds.). Plenum Press, New York. pp. 169-197.

Hyatt AD, Marshall AT (1985) An alternative microdroplet method for quantitative X-ray microanalysis of biological fluids. Micron and Microscopica Acta **16**: 39-44.

Heinrich KFS (1987) Mass absorption coefficients

for electron probe microanalysis. In: X-ray Optics and Microanalysis. Brown JD, Packwood RH (eds.). University of Western Ontario, London, Canada. pp. 67-119.

Hemens CM, Haythornthwaite RF, Nandi BN (1990) Energy-dispersive X-ray microprobe analysis of materials containing light elements using peak ratios. Scanning **12**: 253-256.

Johnson D, Izutsu K, Cantino M, Wong J (1988) High spatial resolution microscopy in the elemental microanalysis and imaging of biological systems. Ultramicroscopy **24**: 221-236.

L'Esperance G, Botton G, Caron M (1990) Detection and quantification problems in the analysis of light elements with UTW detectors. Microbeam Analysis **1990**. San Francisco Press. pp. 284-288.

LeFurgey A, Davilla SD, Kopf DA, Sommer JR, Ingram P (1992) Real-time quantitative elemental analysis and mapping: microchemical imaging in cell physiology. J Microsc **165**: 191-223.

Lowe BG (1989) Problems associated with EDX detectors from a manufacturer's point of view. Ultramicroscopy **28**: 150-156.

Marshall AT (1980) Freeze-substitution as a preparation technique for biological X-ray microanalysis. Scanning Electron Microsc **1980**;II: 395- 408.

Marshall AT (1982) Applications of $\phi(\rho z)$ curves and a windowless detector to the quantitative X-ray microanalysis of frozen-hydrated bulk biological specimens. Scanning Electron Microsc. **1982**;1: 243-260.

Marshall AT (1984) The windowless energy dispersive detector: prospects for a role in biological X-ray microanalysis. Scanning Electron Microsc. **1984**;II: 493-504.

Marshall AT (1987) Scanning electron microscopy and X-ray microanalysis of frozen-hydrated bulk samples. In: Cryotechniques in Biological Electron Microscopy. Steinbrecht RA, Zierold K (eds.). Springer Verlag, Berlin. pp. 240-257.

Marshall AT (1989) Intracellular and luminal ion concentrations in sea turtle salt glands determined by X-ray microanalysis. J Comp Physiol **159**: 609-617.

Marshall AT, Condron RJ (1987) A simple method of using $\phi(\rho z)$ curves for the X-ray microanalysis of frozen-hydrated bulk biological samples. Micron and Microscopica Acta **18**: 23-26.

Marshall AT, Wright O (1991) Freeze-substitution of scleractinian coral for confocal scanning laser microscopy and X-ray microanalysis, J Microsc **162**: 341-354.

Marshall AT, Hyatt AD, Phillips JG, Condron RJ (1985) Isosmotic secretion in the avian nasal salt gland: X-ray microanalysis of luminal and intracellular ion distributions. J Comp Physiol **156**: 213-227.

Morgan AJ, Winters C (1989) Practical notes on the production of thin aminoplastic standards for quantitative X-ray microanalysis. Micron and Microscopica Acta **20**: 209-212.

Musket RG (1981) Properties and applications of windowless Si(Li) detectors. In: Energy Dispersive X-ray Spectrometry. Heinrich KF, Newbury DE, Myklebust RL, Fiori CE (eds.). Natl Bur Stand Spec Publ **604**, US Dept of Commerce, Washington DC. pp 97-126.

Musket RG (1986) Considerations for application of Si(Li) detectors in analysis of sub-keV, ion-induced X-rays. Nuclear Instruments and Methods in Physics Research **B15**: 735-739.

Nicholson WAP, Gray CC, Chapman JN, Robertson BW (1982) Optimizing thin film X-ray spectra for quantitative analysis. J Microsc **125**: 25-40.

Pallaghy CK (1973) Electron probe microanalysis of potassium and chlorine in freeze-substituted leaf sections of *Zea mays*. Aust J Biol Sci **26**: 1015-1034.

Parobek L, Brown JD (1978) The atomic number and absorption correction in electron probe microanalysis at low electron energies. X-ray Spectrom **7**: 26-30.

Patak A, Wright A, Marshall AT (1993) Evaluation of several common standards for the X-ray microanalysis of thin biological specimens. J Microsc **170**: 265-273.

Philibert J (1963) A method for calculating the absorption correction in electron probe microanalysis. In: X-ray optics and X-ray Microanalysis. Pattee HH, Cosslett VE, Engström A (eds.). Academic Press. pp. 379-392.

Reed SJB (1965) Characteristic fluorescence corrections in electron probe microanalysis. Br J Appl Phys **16**: 913-926.

Reed SJB (1975) Electron Microprobe Analysis. Cambridge Univ. Press, U.K. pp. 1-400.

Roomans GM (1979) Standards for X-ray microanalysis of biological specimens. Scanning Electron Microsc **1979**;II: 649-657.

Roomans GM (1980) Quantitative X-ray microanalysis of thin sections. In: X-ray Microanalysis in Biology. Hayat MA (ed.). University Park Press, Baltimore, MD. pp 401-453.

Roomans GM (1981) Quantitative electron probe X-ray microanalysis of biological bulk specimens. Scanning Electron Microsc. **1981**;2: 345-356.

Roos N, Barnard T (1984) Aminoplastic standards for quantitative X-ray microanalysis of thin sections of plastic-embedded biological material. Ultramicroscopy **15**: 277-286.

Russ JC (1974) The direct element ratio model for quantitative analysis of thin sections. In: Microprobe Analysis as Applied to Cells and Tissues. Hall T, Echlin P, Kaufmann R (eds.). Academic Press. pp. 269-276.

Saubermann AJ (1988) X-ray mapping of frozen hydrated and frozen dried cryosections using electron microprobe analysis. Scanning **10**: 239-244.

Scott VD, Love G (1990) The prospects of a universal correction procedure for quantitative EPMA. Scanning **12**: 193-202.

Sevov S, Degischer HP, August H-J, Wernisch J (1989) A comparison of recently developed correction procedures for electron probe microanalysis. Scanning **11**: 123-134.

Sewell DA, Love G, Scott VD (1985) Universal

correction procedure for electron-probe microanalysis. Part 2: The absorption correction. J Phys D Appl Phys **18**: 1244-1268.

Shuman H, Somlyo AV, Somlyo AP (1976) Quantitative electron probe microanalysis of biological thin sections: methods and validation. Ultramicroscopy **1**: 317-339.

Statham PJ (1984) Accuracy, reproducibility and scope for X-ray microanalysis with Si(Li) detectors. J. de Physique Suppl. **45**: C2-175-C2-179.

Statham PJ (1986) Aspects of quantitative microanalysis of light elements by EDXS. Microbeam Analysis **1986**. San Francisco Press. pp. 281-284.

Statham PJ (1988) Pitfalls and advances in quantitative elemental mapping. Scanning **10**: 245-252.

Statham PJ (1991) Limitations and potential for EDX spectrometry in electron beam instruments. Inst. Phys Conf Ser no **119**. Bristol, U.K. pp. 425-432.

Statham PJ, Pawley JB (1978) New method for particle X-ray microanalysis based on peak to background measurements. Scanning Electron Microsc **1978**;1: 469-478.

Statham PJ, Nashashibi T (1988) The impact of low-noise design on X-ray microanalytical performance. Microbeam Analysis **1988**. San Francisco Press. pp. 50-54.

Sumner AT (1990) Gelatine standards for elemental quantification in biological X-ray microanalysis. Scanning Microsc **4**: 429-438.

Thomas LE (1985) Light-element analysis with electrons and X-rays in a high-resolution STEM. Ultramicroscopy **18**: 173-184.

Discussion with Reviewers

P.J. Statham: Your measurements on C, O and continuum are very interesting since continuum measurement appears to be insensitive to mass loss in some circumstances. How useful are the results in such cases? Do you have any suggestions as to how such measurements could be used to make corrections?
Authors: The continuum signal is insensitive to mass loss in the, perhaps fortuitous, instances where loss is balanced by contamination. Since the total mass of the analysed volume remains the same, the mass fraction of elements which are not lost will also remain the same. It is self evident that analyses of C and O will be in error. I think that if values of the latter are required then the situation can only be monitored by looking at C and O counts over time and avoided. The point is that continuum generation cannot be relied upon to indicate that mass loss and contamination are **not** occurring.

Reviewer I: Was a single spot or a small raster used for the static beam mode, and was drift correction applied?
Authors: Static beam analysis was carried out using rasters as described in the **Methods** section. Drift correction was not used for elemental imaging because this was carried out at low magnifications and error due to drift was not a problem.

Reviewer I: Please comment briefly on the limitations of freeze substitution (FS) for quantitative biological microanalysis. For example, is it possible (or even necessary) to assess the viability of the coral epithelium tissue from K/Na ratios which might be more adversely affected by the FS treatment than P or S?
Authors: To be certain that freeze-substitution preserves diffusible elements in correct absolute concentrations, it is advisable to check by analysis of freeze-dried frozen sections of the same sample. The definitive experiments to demonstrate that loss and/or redistribution of diffusible elements is either avoidable or inevitable have yet to be done. Our own preliminary experiments suggest that redistribution and loss are avoidable. In the case of scleractinian coral there is little choice in the matter of preparation methods, frozen sections are impossible to obtain and intracellular Na and K concentration have not been measured other than in our freeze-substituted preparations. In this paper we are, however, only concerned with elements which are firmly bound in mucocytes. It seems unlikely that lose and redistribution would occur.